IN VIVO BIOLUMINESCENCE IMAGING OF CELL DIFFERENTIATION IN BIOMATERIALS: A PLATFORM FOR SCAFFOLD DEVELOPMENT

Juli R. Bagó , PhD,[1] Elisabeth Aguilar, MS,[1] Maria Alieva, MS,[1] Carolina Soler-Botija, PhD,[2] Olaia F. Vila, MS,[2] Silvia Claros, PhD,[3] Jose´ A. Andrades, PhD,[3] José Becerra, PhD,[3] Nuria Rubio, PhD,[1] and Jerónimo Blanco, PhD[1]

[1]Cardiovascular Research Center CSIC-ICCC, CIBER-BBN, Barcelona, Spain.

[2]ICREC Research Program, Research Institut Fundation for Health Sciences "Germans Trias i Pujol" (IGTP), Badalona, Spain.

[3]Department of Cell Biology, Genetics and Physiology, Faculty of Sciences, Laboratory of Bioengineering and Tissue Regeneration, University of Málaga, CIBER-BBN, Málaga, Spain.

In vivo testing is a mandatory last step in scaffold development. Agile longitudinal noninvasive real-time monitoring of stem cell behavior in biomaterials implanted in live animals should facilitate the development of scaffolds for tissue engineering. We report on a noninvasive bioluminescence imaging (BLI) procedure for simultaneous monitoring of changes in the expression of multiple genes to evaluate scaffold performance in vivo. Adipose tissue-derived stromal mensenchymal cells were dually labeled with Renilla red fluorescent protein and firefly green fluorescent protein chimeric reporters regulated by cytomegalovirus and tissue-specific promoters, respectively. Labeled cells were induced to differentiate in vitro and in vivo, by seeding in demineralized bone matrices (DBMs) and monitored by BLI. Imaging results were validated by RT-polymerase chain reaction and histological procedures. The proposed approach improves molecular imaging and measurement of changes in gene expression of cells implanted in live animals. This procedure, applicable to the simultaneous analysis of multiple genes from cells seeded in DBMs, should facilitate engineering of scaffolds for tissue repair.

Introduction

The objective of tissue engineering (TE) is the production of functional tissue replacements using biological and synthetic materials, often in combination with cells and suitable biochemical factors. Development of materials for bioengineering purposes requires the analysis of multiple of these elements interacting in complex manners. Thus, agile analytical procedures for in vivo evaluation of cell–material interactions would allow scaffold development strategies based on iterative cycles of material production-modification followed by in vivo testing.

The main aim of the current work has been to demonstrate a noninvasive procedure to image differentiation of cells in live animals that should aid in the development of scaffolds for tissue regeneration.

Due to the capacity of visible-light photons to transverse living tissues, bioluminescence imaging (BLI) allows low cost, real-time monitoring of location, proliferation, and differentiation of luciferase-expressing cells in living tissues.[1–6] By using tissue-specific promoters to regulate expression of luciferase reporters introduced in living cells, changes in promoter activity translate into measurable changes in photon fluxes that correlate with transcriptional activity.[7] Thus, noninvasive BLI may be used as a convenient analytical tool to monitor the behavior of cell-seeded biomaterials implanted in live animals.[8]

Demineralized bone matrix (DBM), consisting of acidextracted rat cortical bone allograft,[9,10] provides a convenient testing ground to demonstrate imaging procedures applicable to the

43 development of new materials for bone formation. Porous DBM allows infiltration and
44 colonization by host cells that, instructed by osteoinductive signals and growth factors remaining
45 within the collagen structure, supports osteogenesis. 11,12

46 Correct bone healing requires not only stem cell populations capable of osteogenic differentiation,
47 but also the formation of a vascular bed to support metabolic needs.13 In its absence, the ensuing
48 hypoxia results in cell loss and no formation of bone. Different phenotypic markers can be used
49 to monitor sequential stages during bone formation and healing. Bone gamma-carboxyglutamate
50 protein or osteocalcin (OC), the expression of which is limited to cells of the osteoblasts
51 lineage,14 is the major noncollagenous bone matrix protein expressed in bone. Platelet endothelial
52 cell adhesion molecule-1 (PECAM-1) is a frequently used marker constitutively expressed in
53 endothelial cells, platelets, and specific immune system cells.15 Finally, genes such as lactate
54 dehydrogenase A16 and phosphoglycerate kinase 1 (PGK1)16 can be used as proxy reporters
55 responsive to hypoxia activation during bone formation and healing.

56 Human adipose tissue mesenchymal stromal cells (hAMSCs) have been proposed for bone
57 repairing in TE,17 due to their capacity to differentiate into cell lineages involved in osteogenic
58 and vascular development, ease of isolation, abundance, and long-term stability during in vitro
59 expansion.18

60 In the current work, we labeled hAMSCs with lentiviral vectors for the expression of chimeric
61 photoproteins with two types of activities: bioluminescence for noninvasive BLI and fluorescence
62 for cell enrichment and histological analysis.

63 In addition, to take into consideration the inherently noisy environment of measurements in live
64 animals, we adopted an improved luciferase-labeling strategy, where constitutively active and
65 tissue-specific promoters are simultaneously used to regulate light production by two different
66 luciferases in the same cell. Thus, imaging of constitutively expressed Renilla reniformis
67 luciferase (RLuc), regulated by the cytomegalovirus (CMV) promoter, is used to evaluate the cell
68 number, while imaging of Photinus pyralis luciferase (PLuc), regulated by inducible tissue-
69 specific promoters (PECAM-1,19 OC,20 or hypoxia21), is used to evaluate cell differentiation
70 and hypoxia. In this manner, changes in tissue-specific reporter expression are calculated in
71 relation to the level of constitutive reporter expression, and allow taking into account different
72 types of system's noise, including that resulting from changes in the cell number.

73 We show that this is a convenient and sensitive strategy to noninvasively monitor changes in
74 tissue-specific gene expression during osteogenesis in vivo that also facilitates subsequent
75 histological validation through fluorescence imaging.

76 **Materials and Methods**

77 *Generation of luciferase-fluorescent protein reporters regulated by a specific human OC*
78 *promoter, human PECAM-1 promoter, and hypoxia-response element promoter*

79 A pLox:PLuc:green fluorescent protein (GFP) lentiviral vector containing a fusion reporter
80 comprising PLuc and GFP was obtained by polymerase chain reaction (PCR) amplification and
81 standard cloning procedures using the PLuc and GFP genes from plasmid pGL4.10:PLuc
82 (Promega Corporation) and pEGFP-N1 plasmid (Clontech Lab.). PLuc was amplified from
83 pGL4.10:PLuc using paired primers:
84 5'-CTCGAGATGGAAGATGCCAAAAACATTAAGAAG-3' and
85 5'-AGATCTCCATGGAGGCGATCTTGCCGCCCTTC-3' and cloned into the pCR2.11 vector

86 (Invitrogen). After, the PLuc gene was then removed from the pCR2.11 plasmid using NcoI/SpeI
87 enzymes and cloned into the pEGFP-N1 vector cleaved with NcoI/XbaI. Finally, the in-frame
88 fusion reporter gene was excised from the pEGFP-N1 plasmid using EcoRI enzyme and cloned
89 into the EcoR1 site of the pLox lentiviral vector, to obtain the pLox:PLuc:GFP vector.

90 The 800-bp human OCpromoter (hOCp)was PCR-amplified from genomic DNA using specific
91 primers: 5¢-CTGCAGGGT CAGGAGGAGAAT-3¢ and 5¢-GGGCTGCTGCTCAGGACT-3¢ as
92 described16 and cloned into the pCR2.11 vector (Invitrogen). The promoter sequence was then
93 removed from the pCR2.11 vector using XbaI/SpeI enzymes and cloned into the SpeI site of the
94 pLox:PLuc:GFP lentivirus vector. Human PECAM-1 promoter (HPECAM-1p) was kindly
95 provided by Dr. Carmelo Bernabe´u (Centro de Investigaciones Biolo´gicas CSIC, Madrid, Spain)
96 and cloned into pLox:PLuc:GFP using XbaI/SpeI and SpeI enzymes, respectively. The hypoxia-
97 response element promoter (HRE-12p) artificial promoter was constructed as described.17
98 Briefly, two self-complementary 79 oligonucleotide sequences corresponding to the HRE-binding
99 sequence of lactate dehydrogenase A (LDHA), phosphoglycerate kinase 1 (PGK1), and enolase 1
100 (ENO1) were annealed to generate a dsDNA monomer fragment with XbaI- and SpeI-compatible
101 cohesive ends. After self-ligation of this monomer and agarose gel electrophoresis, a repetition of
102 12 monomers was selected from the gel and cloned into the SpeI site of the pLox:PLuc:GFP
103 lentivirus vector.

104 The CMV:RLuc:RFP:ttk lentiviral vector containing a trifunctional chimeric construct
105 comprising the RLuc reporter gene, the monomeric red fluorescent protein (RFP), and a truncated
106 version of the herpes simplex virus thymidine kinase gene sr39tk (ttk) under transcriptional
107 control of CMV was a kind gift of Professor S.S Gambhir (Dept. Radiology, Stanford University,
108 US).

109 *Lentiviral particle production*

110 Viral particles were produced in human embryonic kidney cells 293T grown in Dulbecco's
111 modified Eagle's mediumhigh glucose (DMEM-hg; Sigma), 10% heat-inactivated fetal bovine
112 serum (FBS; Sigma), 2mM l-glutamine (Sigma), 50 units/mL penicillin/streptomycin (Sigma),
113 and 2mMHepes. The day before transfection, 3 106 trypsinized cells were seeded on 10-cm2 poly-
114 d-lysine-treated plates (Sigma). Previously described lentiviral transfer vector DNA (PLoxhOCp:
115 PLuc:GFP;   PLox-hPECAM-1p:PLuc:GFP;   PLox-HRE-   12p:PLuc:GFP;   and
116 CMV:hRLuc:RFP:ttk) (15 mg) was mixed with viral envelope plasmid (pMD-G-VSV-G, 5 mg),
117 packaging construct (pCMV DR8.2, 10 mg), 450 mL of water, and 50 mL of 2.5M CaCl2, and
118 then added dropwise to 500 mL of Hepes-buffered saline 2 (pH 7) and incubated at room
119 temperature for 20 min. This DNA solution was then added dropwise to the plate containing the
120 293T cells in a growth medium, swirled gently, and then incubated for 16 h at 37ºC with 5% CO2.
121 The following day, the transfection solution was removed, and the cells were rinsed with
122 phosphatebuffered saline (PBS) 1, and the medium without FBS was added to the cells. After a
123 48-h incubation, the supernatant was collected, centrifuged at 400 g to remove cell debris, and
124 filtered through a 0.45-mm low-protein-binding filter (Corning). The filtered supernatant was then
125 loaded in thin-wall polyallomer tubes and ultracentrifuged using the SW41.Ti rotor at 26,000 rpm
126 for 90 min at 4C in a L-100XP (Beckman Coulter) ultracentrifuge. The virus pellets were
127 resuspended in PBS and kept at - 80C for storage. Viral titers were determined using the HIV-1
128 p24 antigen EiA (Beckman Coulter) 96 test kit.

129 *hAMSC transduction and differentiation*

hAMSCs were isolated from adipose tissue derived from cosmetic subdermal liposuctions, with patient consent. Liposuction samples were obtained after written informed consent by anonymous donors from Hospital de la Santa Creu i Sant Pau, Barcelona, Spain. Work with human samples was approved by written consent by the Ethics Committee of Clinical Investigation of Hospital Santa Creu i Sant Pau, Barcelona, Spain; and Bioethics Subcommittee of Superior Council of Scientific Research. Briefly, lipoaspirate was suspended in 1 collagenase type I (Invitrogen) solution and incubated at 37C and inactivated by addition of DMEM+ 10% FBS. hAMSCs were isolated by plastic adherence technique. hAMSCs were grown in DMEM-hg with 20% FBS (Hyclone), 2mM l-glutamine (Sigma), and 50 units/mL penicillin/streptomycin (Sigma), expanded for until 70% of, and frozen at passage 2. Three-donor pool at passage 4 was used for the study.

hAMSCs were transduced using CMV:hRLuc:RFP:ttkconcentrated lentiviral stock (2 · 106 transduction units/mL, multiplicity of infection [MOI] = 21) during 48 h. The highest 11% RFP-expressing cells were selected by fluorescenceactivated cell sorting (FACS). Sorted cells were divided in three aliquots and transduced again with either concentrated lentiviral PLox-hOCp:PLuc:GFP, PLox-HRE-12p:PLuc:GFP or PLox-hPECAM-1p:PLuc:GFP stocks (2 · 106 transduction units/mL, MOI = 21) during 48 h to obtain double-transduced cells hOCp:PLuc:GFP/CMV:RLuc:RFP:ttk-hAMSCs (hOCp: hAMSCs), HRE-12p:PLuc$GFP/CMV:RLuc:RFP:ttk-hAMSCs (HRE-12p:hAMSCs), and hPECAM-1p:PLuc$GFP/CMV: RLuc:RFP:ttk-hAMSCs (hPECAM-1p:hAMSCs), respectively.

For in vitro osteogenic differentiation, cells were cultured in a StemPro Osteogenesis Differentiation Kit (Gibco) during a 14-day period, following the manufacturer's instructions. For in vitro endothelial differentiation, cells were cultured in Endothelial Cell Growth Medium-2 (Lonza) during a 14-day period. For hypoxia activation, cells were grown under hypoxic conditions in an incubator supplied with 1% O2 during 48 h.

BLI of luciferase activity in vitro

BLI of cultured double-transfected cells hOCp:hAMSCs, HRE-12p:hAMSCs and hPECAM-1p:hAMSCs was performed at the end of the differentiation or hypoxia activation process. For BLI, the medium was removed from plates (24- well plates), and cells were rinsed twice with PBS 1 · and immediately imaged after addition of 100 mL/well of PLuc or RLuc substrate stock reagent (Promega Corporation). PLuc and RLuc activities were imaged in consecutive days. For imaging, a plate was placed in the detection chamber of a high-efficiency ORCA-2BT Imaging System (Hamamatsu Photonics) provided with a C4742-98-LWG-MOD camera fitted with 512 · 512-pixel charge-couple device (CCD) cooled at - 80C. Images were acquired during 30 s using 1 · 1 arrays (binning 1 · 1) for RLuc detection, and during 1min using an 8 · 8 array (binning 8 · 8) for PLuc detection. To register the position of the light signal, an additional image was obtained using a white light from a lamp in the detection chamber. Image analysis was performed using Wasabi software (Hamamatsu Photonics). Recorded light fluxes were expressed as photon counts (PHCs) after discounting background using the formula, PHCs = (total number of PHCs in the area of interest) – ([number of pixels in the area of interest] · [background average PHCs/pixel]).

Arbitrary color scales are used to represent standard light intensity levels for PLuc (blue = lowest; red = highest) and for RLuc (black = lowest; blue = highest).

Cell implantation in DBM chambers and Matrigel

173 Six-week-old severe combined immunodeficiency disease (SCID) mice were purchased from
174 Charles River and maintained in a specific pathogen-free environment throughout the experiment.
175 All animal-related procedures were performed with the approval of the Animal Care Committee
176 of the Cardiovascular Research Center and the Government of Catalonia. Mice were anesthetized
177 by intraperitoneal injection of a mixture containing 100mg/kg ketamine (Merial) and 3.3mg/kg
178 xilacine (Henry Schein). Three DBM chambers were subcutaneously implanted in the backs of
179 six SCID mice 1 week before seeding with cells. DBMs were prepared as described[22] and had
180 the ends sealed with Millipore filters (Millipore Ltd.) to prevent leakage. Trypsinzed cells, $3 \cdot 10^5$
181 suspended in 15 mL of a-MEM, were injected through the mouse skin and the sealed end of the
182 DBM using an insulin syringe. The distribution of DBM chambers in mice is indicated in Figure
183 2A diagram.

184 A mixture of 50 mL Matrigel with $3 \cdot 10^5$ cells suspended in 50 mL of PBS was subcutaneously
185 injected in the paraspinal space of the mouse (four independent injection sites per animal; total n
186 = 2) using a 21–25G-size needle.

187 *RNA extraction and real-time PCR*

188 Total RNA was extracted from DBM scaffolds implanted in mice, at 3-week intervals and from
189 in vitro samples at the end of differentiation or hypoxia activation process. RNA extraction was
190 performed using the RNAeasy mini kit (Qiagen). One mg of total RNA was reverse-transcribed
191 using the Revertaid First Strand cDNA Synthesis Kit (Fermentas), and product cDNA was then
192 real-time PCR-amplified, using ABI PRISM 7000——————————————— (Applied
193 Biosystems). The glyceraldehyde- 3-phosphate dehydrogenase (GADPH) gene was used as an
194 internal control. Due to the low amounts of cDNA obtained from DBM scaffolds, a
195 preamplification stage was performed with TaqMan——————————————— PreAmp
196 Master Mix (Applied Biosystems).

197 FAM-labeled primer/probes were purchased from Applied Biosystems: PECAM-1
198 (Hs00169777_m1), GAPDH (Hs99999905_m1), BGLAP (Hs01587813_g1), LDHA
199 (Hs00855332_g1), and PGK1 (Hs00943178_g1). The threshold cycle (Ct) method was used to
200 quantify relative expression for each gene using GAPDH as endogenous reference.

201 *Noninvasive BLI of luciferase activity from implanted DBMs and Matrigel*

202 For in vivo BLI, anesthetized mice bearing DBMs seeded with PLuc-expressing cells were
203 intraperitonally injected with 150 mL of luciferin (16.7mg/mL in physiological serum; Braun).
204 Alternatively, for in vivo BLI of RLuc-expressing cells, mice were intravenously (tail vein)
205 injected with 25 mL of benzyl coelenterazine (hCTZ, 1mg/mL in 50/50 propylene glycol/ethanol;
206 Nanolight Technology, www.nanolight .com) diluted in 125 mL of water.

207 PLuc and RLuc activities were imaged in consecutive days. Images were acquired during 5 min.
208 In all cases, an additional image of the animal was obtained using a whitelight source inside the
209 detection chamber, to register the position of the luminescence signal in the animal.

210 To increase detection sensitivity, readout noise of the recorded signal was reduced by
211 simultaneous reading of light events recorded in arrays of $8 \cdot 8$ adjacent pixels (binning $8 \cdot 8$) in
212 the camera CCD. Mice were monitored during the 8- week period for DBMs and during 6 days
213 for Matrigel at the indicated times. The photons recorded in images were quantified and analyzed
214 using Wasabi image analysis software (Hamamatsu Photonics).

215 *Fluorescence angiography and confocal microscope localization of hAMSCs in DBMs*

216 An fluoresceinisothiocyanate (FITC)-conjugated high-MW (2,000,000 Da) dextran, FITC-
217 dextran (Sigma), was used as a fluorescent tracer of microvascular structures in DBM scaffolds.
218 FITC-dextran 200 mL (10 mg/mL) was injected through the lateral tail vein of anesthetized mice.
219 Ten minutes after inoculation, mice were sacrificed, DBM chambers retrieved and fixed in 10%
220 formalin solution (Sigma) during 24 h, and sectioned for microscopy. Laser confocal microscopy
221 was used to analyze microvascular structures connected to the host vascular system in DBMs and
222 their relationship with implanted fluorescent-labeled hAMSCs. Three DBMs were retrieved and
223 analyzed at 3-week intervals.

224 *Histological analysis*

225 DBM chambers were retrieved from sacrificed animals at days 21, 42, and 56 postimplantation
226 and were fixed in 10% formalin solution (Sigma) for 24 h. The chambers were then decalcified
227 and dehydrated before embedding in paraffin. Blocks were sectioned into slices of 5-mm
228 thickness and stained by hematoxylin and eosin (H&E). Immunofluorescence stain samples were
229 incubated with the primary antibodies against HIF1-a, hOC (5 mg/mL), or hPECAM-1 (4 mg/mL;
230 Abcam). Secondary antibody conjugated with Cy5 (3 mg/mL; Jackson ImmunoResearch) was
231 applied, and sections were counterstained with 4,6-diamidino-2- phenylindole (Hoechst, Sigma).
232 The signal was visualized with confocal laser scanning microscopy (Leica TS1 SP2). For anti-
233 human CD31 immunostaining, samples were incubated with mouse monoclonal antibody, anti-
234 human CD31 (DAKO; dilution 1:50). Secondary antibody conjugated with biotin anti-mouse
235 (Vector Laboratories; dilution 1:200) was added, and after color reaction with 3,3-
236 diaminobenzidine tetrahydrochloride (DAB) solution, contrast staining was conducted using
237 hematoxylin.

238 *Statistical analysis*

239 Statistical analysis was performed using a two-tailed Student's t-test. Values are presented as
240 mean – s.d. One-way ANOVA with Tukey B post hoc analysis was applied to determine
241 significance among more than 2 groups. Descriptive statisticswere performedwith SPSS Statistics
242 (15.0.1 version; SPSS Inc.). Statistical tests were considered significant when $p < 0.05$.

243 **Results**

244 *HRE-12p-, hPECAM-1h-, and hOCp-regulated photoproteins can be used as reporters of hypoxia*
245 *state, endothelial, and osteogenic differentiation in vitro*

246 Expression of hPECAM-1p-, hOCp-, or HRE-12p-regulated genes is an indicator of cell
247 differentiation to the endothelial and osteoblastic lineages and hypoxic state.

248 To show that PECAM-1-, OC-, and HRE-promoter driven expression of photoprotein reporters
249 can be used to monitor endogenous gene expression, hAMSCs were transduced as described in
250 the Materials and Methods section using lentiviral vector constructs described in Figure 1A.

251 To analyze the relationship between expression of endogenous hypoxia response, PECAM-1 and
252 OC genes, and light production driven by the corresponding promoters, photoreporter-transduced
253 cells were grown either under normoxic or hypoxic conditions, in control media and
254 differentiation- inducing media, and analyzed by BLI to determine PLuc and RLuc activities (Fig.
255 1B, C left). After BLI, mRNA was extracted for real-time PCR analysis (Fig. 1C right).

256 HRE-12p:hAMSCs grown during 48 h under hypoxic conditions (1% O2) in a control medium
257 showed a ratio of PLuc to RLuc activity 5.5-times higher than that of cells grown under normoxic

258 conditions (20% O2), while expression of hypoxia-induced genes PGK1 and LDH, measured by
259 real-time PCR, was twofold higher under hypoxic than under normoxic conditions.

260 After a 14-day period of growth in an either differentiation- inducing or control medium,
261 hPECAM-1p:hAMSCs grown in an endothelial differentiation medium showed a ratio of PLuc
262 to RLuc activities 3.5-times higher than that of control cells, while hOCp:hAMSCs grown in an
263 osteogenicinducing medium showed a ratio of PLuc to RLuc activities 2.6-times higher than that
264 of control cells (Fig. 1C). Real-time PCR quantification of mRNA from the same cells, after BLI
265 analysis, showed a similar trend, and the level of PECAM-1 and OC expression was 13-fold and
266 17-fold higher in cells induced to differentiate to the endothelial and osteogenic lineages,
267 respectively, than that of undifferentiated cells. In all cases, differences were statistically
268 significant. Thus, in the three independent cases, changes in the expression of a specific promoter
269 regulated luciferase and reflected changes in the expression of the corresponding endogenous
270 promoter-regulated gene.

271 *Noninvasive BLI monitoring of hypoxia activation, endothelial, and osteogenic differentiation of*
272 *hAMSCs seeded in DBM scaffolds in SCID mice*

273 We used DBM as an established model of biomaterial scaffold that provides an osteoinductive
274 environment to demonstrate the use of BLI for noninvasive analysis of changes in gene expression
275 in live mice. To do this, hAMSCs double transduced with the inducible and constitutive
276 photoprotein reporters were seeded in DBM matrices implanted in the backs of six SCID mice
277 (three DBM chambers/mice), according to the diagram in Figure 2A, and regularly imaged during
278 a 56-day period (Fig. 2A).

279 Quantification of PHCs from the hAMSCs in the scaffolds shows that the ratio PLuc/RLuc
280 activity (Fig. 2B) changed by 125-fold (day 28) for hPECAM-1p (Fig. 2B.2) regulated luciferase,
281 and by 15-fold (day 35) for hOCp (Fig. 2B.3) regulated luciferase, both relative to the day of
282 implantation (day 0), indicative of the changes in gene expression associated with differentiation
283 to the endothelial and osteogenic lineages, respectively. In the case of scaffolds seeded with
284 hAMSCs expressing an HRE-12p regulated luciferase, the ratio PLuc/ RLuc achieved no
285 significant increase by 56 days (Fig. 2B.1).

286 Real-time PCR was also used as independent procedure, to analyze mRNA extracted from the
287 hAMSCs seeded in DBMs at days 21, 42, and 56, and validate BLI data. Changes in levels of
288 PECAM-1, OC, PGK1, and LDHA gene expression are shown in Table 1. At the indicated days,
289 mRNA levels were 8.86, 9.41, and 18.85-fold for PECAM-1, and 5.48-fold, 9.96-fold, and 22.34-
290 fold for OC, relative to those from hAMSCs grown in a noninducing medium during the same
291 time period. Also in agreement with BLI data, the modest, not significant, increase in HRE-12p-
292 regulated luciferase expression correlated with a nondetectable change in the level of mRNA
293 expression of two genes, PGK1 and LDHA that are upregulated under hypoxic conditions.

294 Thus, in vivo, changes in the activity of PLuc regulated by promoters of genes that are expressed
295 in osteogenic and endothelial cell lineages or during hypoxia correlate with changes in the levels
296 of mRNA expression for the corresponding endogenous promoter-regulated gene, supporting the
297 use of BLI to noninvasively report changes in gene expression.

298 *Angiogenesis in hAMSC seeded DBM scaffolds in live mice*

299 To visualize development of microvasculature in the implanted DBMs, at days 19, 30, and 56
300 postimplantation, mice were perfused by injection trough the lateral tail vein with a high-

molecular-weight (2,000,000 Da) dextran–fluorescein conjugate (Fig. 3A). After harvesting, perfused DBMs were lightly fixed in formaldehyde, sectioned, and prepared for imaging by laser confocal microscopy (see Supplementary Video S1 online; Supplementary Data are available online at www.liebertpub.com/tea).

As shown in Figure 3B, DBMs harvested by day 21 and thereafter were fluorescent, and fluorescence intensity was directly proportional to the elapsed time after implantation ($5.15 \cdot 108$, $6.67 \cdot 108$, and $8.06 \cdot 108$ p/s/cm2/sr for days 21, 42, and 56* days, respectively *$p < 0.005$), indicative of the existence of a vascular system, well connected to that of the host. The fluorescent capillary bed connected to the host vascular system that invaded the DBM matrix could be easily visualized by low-magnification confocal microscopy of DBM sections. To localize the hAMSCs originally seeded in DBMs, we further exploited the inclusion of fluorescent protein activities associated with the luciferases in the chimeric photoreporters. Confocal microscope observation at high magnification showed, in all cases, the presence of red fluorescent cells within the DBM matrix (Fig. 3C), corresponding to hAMSCs constitutively expressing RFP regulated by the CMV promoter. Moreover, in the case of DBMs seeded with hPECAM-1p:hAMSCs, red fluorescent cells frequently expressed green fluorescence, indicating endothelial differentiation (shown as yellow in composite images) (Fig. 3C and Supplementary Video S2 online). What is more, such cells had endothelial morphology and were found lining thin vascular structures filled with dextran. Additional support for the endothelial lineage of these cells was obtained by staining with an antihuman-PECAM-1-specific antibody, conjugated to a Cy5 fluorescent second antibody, chosen to generate a far-red fluorescent signal, easily distinguishable from that of the RFP signal (Fig. 4B).

In the case of DBMs seeded with hOCp:hAMSCs, the implanted red fluorescent cells also expressed green fluorescence (appearing yellow in composite images) (Fig. 3C). However, in this case, the cell phenotype was not endothelial, but corresponded with that of cells from the osteogenic lineage, and green cells did not appear associated with vascular structures. In addition, the green fluorescent cells stained positively with an antihuman-OC-specific monoclonal antibody, conjugated to a Cy5 fluorescent second antibody, providing further evidence of their osteogenic lineage (Fig. 4C).

Our assessment showed that most of eGFP-expressing cells also expressed RFP, ruling out CMV promoter silencing as the cause for the decrease in production RLuc. Moreover, to ascertain that the increase in the ratio PLuc/RLuc observed by BLI was not due to silencing of the CMV promoter regulating RLuc:RFP expression, we counted the number of red and green fluorescent cells and only green fluorescent cells (that would be generated if the CMV promoter had been silenced). Our results show that in the 12 sections, the counted 579 cells were red + green simultaneously, and only 14 (2.4%) were only green fluorescent (Supplementary Table S1).

Finally, in serial sections from DBMs seeded with HRE- 12p:hAMSCs, contained red fluorescent cells, which showed no green fluorescence (Fig. 3C), indicating that few, if any, of the seeded hAMSCs were under hypoxic stress, in support of the BLI and real-time PCR data. This result was further supported by the absence of cells that stained with an anti- HIF1-a monoclonal antibody, conjugate to a Cy5-labeled second antibody (Fig. 4A).

Moreover, the DBMs were extracted from mice at the end of the BLI experiment, sectioned, and stained with anti human- PECAM antibody (Fig. 4D) and H&E (Fig. 4E) to show vascular structures and calcium deposits indicative of bone formation. After, parallel sections from the

345 same location were also imaged by laser confocal microscope to determine the presence of red
346 and green fluorescent cells.

347 Our results show vascular-like structures in the DBM interior that stain with anti-hPECAM
348 antibody and correspond with cells that expressed RFP and eGFP regulated by the PECAM
349 promoter in parallel sections. Also, H&E-stained DBM sections showed purple-staining calcium
350 deposits that also corresponded with cells expressed RFP and eGFP regulated by the OC promoter
351 in parallel sections. Number of demineralized bone matrix implanted and mice in time is
352 represented in Supplementary Table S2. To show that osteoblastic differentiation is specific of
353 DBM and does not take place in other nonosteoinductive materials, hAMSCs expressing fivefly
354 luciferase regulated by either the OC or the PECAM promoters (as a positive control) were seeded
355 in Matrigel, a proangiogenic material, subcutaneous implanted in the back of SCID mice and
356 monitored during a 6 day period (Supplementary Figure S1).

357 **Discussion**

358 Development of TE strategies proceeds through multiple stages, including material design, in
359 vitro testing, and in vivo demonstration of effectiveness. This complex process would benefit
360 from agile longitudinal noninvasive real-time monitoring of biomaterial–stem cell interactions in
361 live animals. Noninvasive imaging is particularly suited to evaluate the performance of cells in
362 vivo, and could be integrated in design strategies based on iterative cycles of material engineering,
363 in vivo testing, and re-engineering aimed at improving the performance of scaffolds.

364 In the current work, we demonstrate an improved procedure to noninvasively image and measure
365 changes in the expression of several genes during differentiating cells seeded in a model
366 biomaterial implanted in live mice.

367 The physicochemical and instrumental aspects of bioluminescence and its measurement are well
368 established and relatively easy to control in isolated enzymatic systems and cells in vitro.[23,24]
369 However, noninvasive BLI of cells implanted in live animal models presents additional challenges
370 resulting from local differences in the physiological environment and optical properties of
371 intervening tissues that difficult a quantitative analysis of cell behavior.

372 To minimize the effect of these issues during noninvasive analysis of cell differentiation, we use
373 a simple imaging strategy based on labeling the same therapeutic cell with a reference luciferase–
374 fluorescent protein (RLuc-RFP) regulated by a constitutively active promoter, and with a different
375 luciferase–fluorescent protein combination (PLuc-GFP) regulated by the promoter of the target
376 gene we wish to investigate (specific reporter). This double luciferase approach facilitates
377 interpretation of inherently noisy in vivo reporter data, on a per cell basis, for example,
378 independently of the proliferation state of the implanted cells. In addition, the use of chimeric
379 luciferase–fluorescent protein reporters allows both, the selection of reporter expressing cells after
380 labeling and the validation of in vivo imaging data by standard histological procedures.

381 We established that luciferase expression regulated by tissue-specific promoters could be used as
382 correlates of endogenous gene activity. In hAMSCs dually labeled to express tissue-specific
383 promoter- (hOCp, hPECAM-1p, and HRE-12p) regulated PLuc, and CMV-regulated RLuc, and
384 induced to differentiate in vitro, the ratio of PLuc/RLuc activity was statistically significantly
385 higher (2.6, 3.5, and 5.5 times, respectively) than that of control, uninduced cells. These changes
386 in luciferase activity correlated with changes in mRNA levels for the corresponding genes
387 regulated by the endogenous promoters (17-fold, 13-fold, and 2-fold, respectively) in the same
388 induced cells, as verified by an independent procedure using real-time PCR.

389 Differences in the trends of BLI and real-time PCR values may reflect the inevitable use
390 abbreviated promoter constructs with structures not entirely corresponding to those of the
391 endogenous ones, or the insertion of the reporter constructs at random chromosomal locations.

392 Due to the preservation of the three-dimensional, as well as molecular, information in DBM, this
393 material is a convenient scaffold model in which to demonstrate the capacity to in vivo image
394 changes in gene expression during bone development.

395 hAMSCs labeled to express luciferases regulated by tissuespecific and constitutively active
396 promoters were seeded in DBMs subcutaneously implanted in the back of SCID mice and imaged
397 weekly during a 56-day period. In these experiments, imaging data showed that there was an
398 increase in the ratio PLuc/RLuc indicative of differentiation of the implanted hAMSCs to the
399 osteogenic and endothelial cell lineages (dynamic range of 15-fold and 125-fold, respectively).
400 However, there was only a slight, not statistically significant, increase in the level of HRE
401 promoter-regulated PLuc, indicative of little hypoxia-related stress in the environment of the
402 implanted cells. Analysis by real-time PCR of mRNA levels in DBMs at specific times during the
403 experiment showed also significant increases in the expression of OC and PECAM-1 genes
404 (dynamic range of 22.3-fold and 18.8-fold, respectively), but not of hypoxia-induced genes, again
405 in agreement with BLI data.

406 Interestingly, in vivo PLuc/RLuc ratios were higher than those found in vitro. This could result,
407 in part, from animal tissues having a higher opacity to the shorter wavelength of RLuc-generated
408 photons (480 l), than to longer-wavelength PLuc photons (578 l). However, probably more
409 important is the fact that DBMs were implanted in a physiological environment, and that their
410 natural origin provides a nearly optimum combination of the structural and molecular cues
411 required to induce cell differentiation.

412 Inoculation of mice at different times of the experiment with a high-MW fluorescent dextran
413 followed by confocal microscope imaging revealed a complex capillary network, functionally
414 connected to the host vascular system that colonizes the DBMs. Within the invading vascular
415 structures, hAMSCs seeded in DBMs appeared to have differentiated to endothelial and
416 osteoblastic lineages as shown by the presence of simultaneously red and green fluorescent cells.
417 In the case of hPECAM-1:hAMSCs, red and green fluorescent cells had spindle shapes and were
418 found in close association lining the capillaries, while in the case of hOCp:hAMSCs, red and
419 green fluorescent cells were found scattered through the material, but not in association with
420 capillaries.

421 Further support that DBM-seeded hAMSCs had differentiated to the endothelial and osteoblastic
422 lineages was provided by their staining with antibodies against PECAM-1 and OC proteins.

423 Small changes in BLI-detectable luciferase activity regulated by the HRE promoter in vivo
424 correlated with the absence of GFP-expressing RFP cells, no increase in the expression of
425 hypoxia-inducible gene mRNA levels, the absence of cells detectable with an anti HIF-a ab, and
426 with the presence of a host capillary network penetrating the scaffolds, to provide necessary
427 oxygen and nutrients.

428 In summary, we show that differentiation of cells seeded in biomaterials implanted in live animals
429 can be reliably monitored using BLI by introducing in the target cells' two different luciferase
430 reporters, one of them regulated by a tissue-specific promoter and the other regulated by a
431 constitutively expressed promoter. By measuring the change in activity of the tissue-specific
432 reporter relative to that of the constitutively expressed reference reporter, it is possible to obtain

information on changes in gene expression relative to an internal standard indicative of cell number, free of artifacts produced by cell death or proliferation. Moreover, by including both reporters in the same cell, noise resulting from uneven distribution of cells with different labels is largely avoided, and comparison between different samples is facilitated. An additional advantage of the reporter strategy was the use of chimeric luminescent/fluorescent reporters. This approach had a double advantage, allowing the use of FACS for purification of labeled cells, previous to seeding in scaffolds, and providing very convenient fluorescent tracers for histological detection of implanted and differentiated cells after in vivo BLI analysis.

Although in the current work we demonstrate the use of three different inducible promoters to regulate a luciferase, there is no limit in the number of genes that could be simultaneously monitored in different samples of biomaterial. Moreover, the availability of additional luciferases with different substrate requirements would allow increasing the number of gene activities that could be monitored in the same cell, or biomaterial sample, widening the scope of biological parameters that could be monitored during scaffold development.

Conclusions

Dual labeling of hAMSCs with constitutively active and tissue-specific promoter-regulated luciferase reporters allows quantitative noninvasive BLI monitoring of gene expression during vascular and bone differentiation, which is independently validated by molecular and histological procedures. This approach could be the basis of an optimization procedure based on iterative cycles of modification–validation for scaffold development.

Acknowledgments

Disclosure Statement

No competing financial interests exist.

References

1. Vilalta, M., Degano, I.R., Bago, J., Gould, D., Santos, M., Garcia-Arranz, M., et al. Biodistribution, long-term survival, and safety of human adipose tissue-derived mesenchymal stem cells transplanted in nude mice by high sensitivity non-invasive bioluminescence imaging. Stem Cells Dev 17, 993, 2008.

2. Degano, I.R., Vilalta, M., Bago, J.R., Matthies, A.M., Hubbell, J.A., Dimitriou, H., et al. Bioluminescence imaging of calvarial bone repair using bone marrow and adipose tissuederived mesenchymal stem cells. Biomaterials 29, 427, 2008.

3. Dothager, R.S., Flentie, K., Moss, B., Pan, M.H., Kesarwala, A., and Piwnica-Worms, D. Advances in bioluminescence imaging of live animal models. Curr Opin Biotechnol 20, 45, 2009.

4. De Boer, J., van Blitterswijk, C., and Lo¨wik, C. Bioluminescent imaging: emerging technology for non-invasive imaging of bone tissue engineering. Biomaterials 27, 1851, 2006.

5. Olivo, C., Alblas, J., Verweij, V., Van Zonneveld, A.J., Dhert, W.J., and Martens, A.C. In vivo bioluminescence imaging study to monitor ectopic bone formation by luciferase gene marked mesenchymal stem cells. J Orthop Res 26, 901, 2008.

6. Geuze, R.E., Prins, H.J., O¨ner, F.C., van der Helm, Y.J., Schuijff, L.S., Martens, A.C., et al. Luciferase labeling for multipotent stromal cell tracking in spinal fusion versus ectopic bone tissue engineering in mice and rats. Tissue Eng Part A 16, 3343, 2010.

7. Chen, I.Y., Gheysens, O., Ray, S., Wang, Q., Padmanabhan, P., Paulmurugan, R., et al. Indirect imaging of cardiacspecific transgene expression using a bidirectional two-step transcriptional amplification strategy. Gene Ther 17, 827, 2010.

8. Vilalta, M., Jorgensen, C., Degano, I.R., Chernajovsky, Y., Gould, D., Noel, D., et al. Dual luciferase labelling for noninvasive bioluminescence imaging of mesenchymal stromal cell chondrogenic differentiation in demineralized bone matrix scaffolds. Biomaterials 30, 4986, 2009.

9. Walsh, W.R., and Christiansen, D.L. Demineralized bone matrix as a template for mineral organic composites. Biomaterials 16, 1363, 1995.

10. Galus, R., W1odarski, P., and W1odarski, K. Influence of fluvastatin on bone formation induced by demineralized bone matrix in mice. Pharmacol Rep 58, 443, 2006.

11. Landesman, R., and Reddi, A.H. In vivo analysis of the halflife of the osteoinductive potential of demineralized bone matrix using diffusion chambers. Calcif Tissue Int 45, 348, 1989.

12. Harakas, N.K. Demineralized bone-matrix-induced osteogenesis. Clin Orthop Relat Res 239, 1984.

13. Santos, M.I., and Reis, R.L. Vascularization in bone tissue engineering: physiology, current strategies, major hurdles and future challenges. Macromol Biosci 10, 12, 2010.

14. Briot, K., and Roux, C. Biochemical markers of bone remodeling. Gynecol Obstet Fertil 33, 1009, 2005.

15. Newman, P.J., and Albelda, S.M. Cellular and molecular aspects of PECAM-1. Nouv Rev Fr Hematol 34 Suppl, S9, 1992.

16. Semenza, G.L., Jiang, B.H., Leung, S.W., Passantino, R., Concordet, J.P., Maire, P., et al. Hypoxia response elements in the aldolase A, enolase 1, and lactate dehydrogenase A gene promoters contain essential binding sites for hypoxiainducible factor 1. J Biol Chem 271, 32529, 1996.

17. Tapp, H., Hanley, E.N., Jr., Patt, J.C., and Gruber, H.E. Adipose-derived stem cells: characterization and current application in orthopaedic tissue repair. Exp Biol Med (Maywood) 234, 1, 2009.

18. Kern, S., Eichler, H., Stoeve, J., Kluter, H., and Bieback, K. Comparative analysis of mesenchymal stem cells from bone marrow, umbilical cord blood, or adipose tissue. Stem Cells 24, 1294, 2006.

505   19. Almendro, N., Bellon, T., Rius, C., Lastres, P., Langa, C., Corbi, A., et al. Cloning of the human platelet
506   endothelial cell adhesion molecule-1 promoter and its tissue-specific expression. Structural and
507   functional characterization. J Immunol 157, 5411, 1996.

508   20. Yeung, F., Law, W.K., Yeh, C.H., Westendorf, J.J., Zhang, Y., Wang, R., et al. Regulation of human
509   osteocalcin promoter in hormone-independent human prostate cancer cells. J Biol Chem 277, 2468,
510   2002.

511   21. Razorenova, O.V., Ivanov, A.V., Budanov, A.V., and Chumakov, P.M. Virus-based reporter systems for
512   monitoring transcriptional activity of hypoxia-inducible factor 1. Gene 350, 89, 2005.

513   22. Nimni, M.E., Bernick, S., Ertl, D., Nishimoto, S.K., Paule, W., Strates, B.S., et al. Ectopic bone
514   formation is enhanced in senescent animals implanted with embryonic cells. Clin Orthop Relat Res 255,
515   1988.

516   23. Giguere, V. Application of the firefly luciferase reporter gene. Methods Mol Biol 7, 237, 1991.

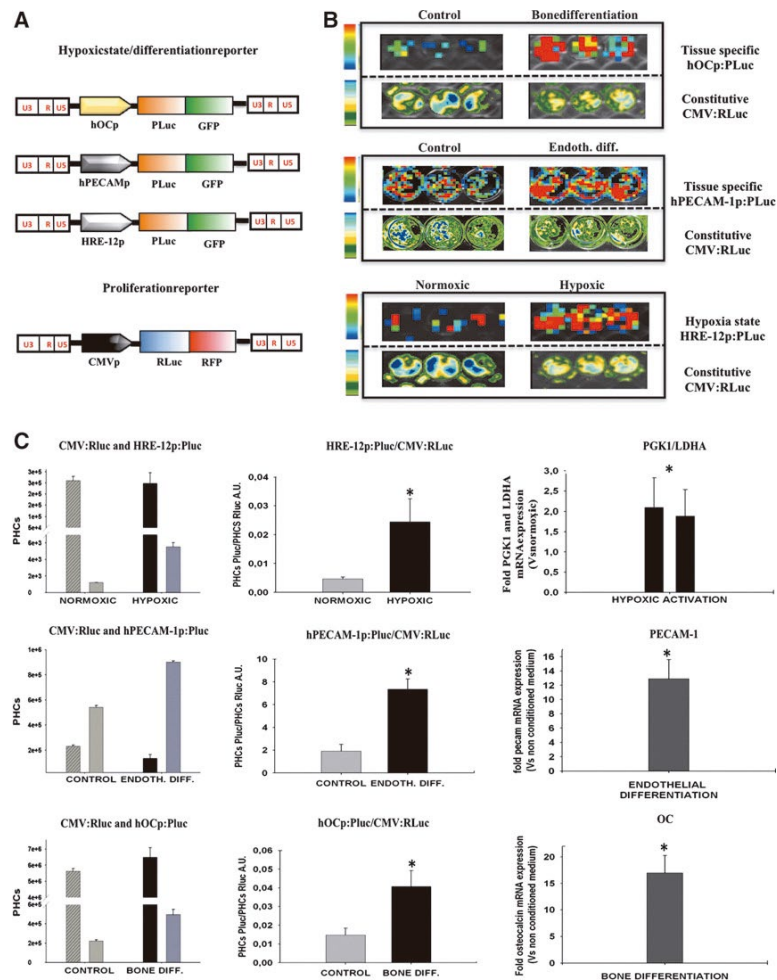517   24. Meager, A. Biological assays for interferons. J Immunol Methods 261, 21, 2002.

FIG. 1. In vitro activity of luciferase reporters regulated by thehuman PECAM-1 promoter (hPECAM-1p), humanOCpromoter (hOCp), or hypoxia-response element promoter (HRE-12p) promoters correlates with mRNA levels for the corresponding endogenous genes. Human adipose tissue mesenchymal stromal cells (hAMSCs) transduced to express Renilla reniformis luciferase (RLuc) regulated by the cytomegalovirus (CMV) promoter and Photinus pyralis luciferase (PLuc) regulated by either hOCp, hPECAM-1p, or HRE-12p promoters were grown under inducing conditions and analyzed by bioluminescence imaging (BLI) to image luciferase activities. After BLI, expression of platelet endothelial cell adhesion molecule-1 (PECAM-1), osteocalcin (OC), phosphoglycerate kinase 1 (PGK1) and LDHA, genes was analyzed by reverse transcription-polymerase chain reaction ofmRNA extracted from the same cells. (A) Diagram showing the luciferase reporter constructs used for cell transductions. (B) Representative images of luciferase activity fromcells grown in control (left panel) or inducing medium (right panel). Top row, PLuc regulated by specific promoter; bottom row, RLuc regulated by CMV promoter. (C, left panel) Quantification of image data from (B). The histograms show average values for photon counts (PHCs) recorded in images for control cells and induced cells (RLuc regulated by theCMVpromoter, line gray bars for control cells and black for induced cells; PLuc regulated by specific promoters, gray bar for control cells, and dark gray for induced cells). (C, center panel) Histograms showing the ratios of PLuc/RLuc activity calculated from BLI images, (control cells, gray bars; induced cells, black bars). (C, right panel) Histograms showingmRNAlevels from inducedhAMSCs versus uninduced. AU, arbitrary light units. Histograms and bars represent the average of four wells and SD, respectively; *p < 0.05. Arbitrary color bars represent light intensity levels for PLuc (blue, low; red, high) and RLuc (green, low; blue, high). Color images available online at www.liebertpub.com/tea
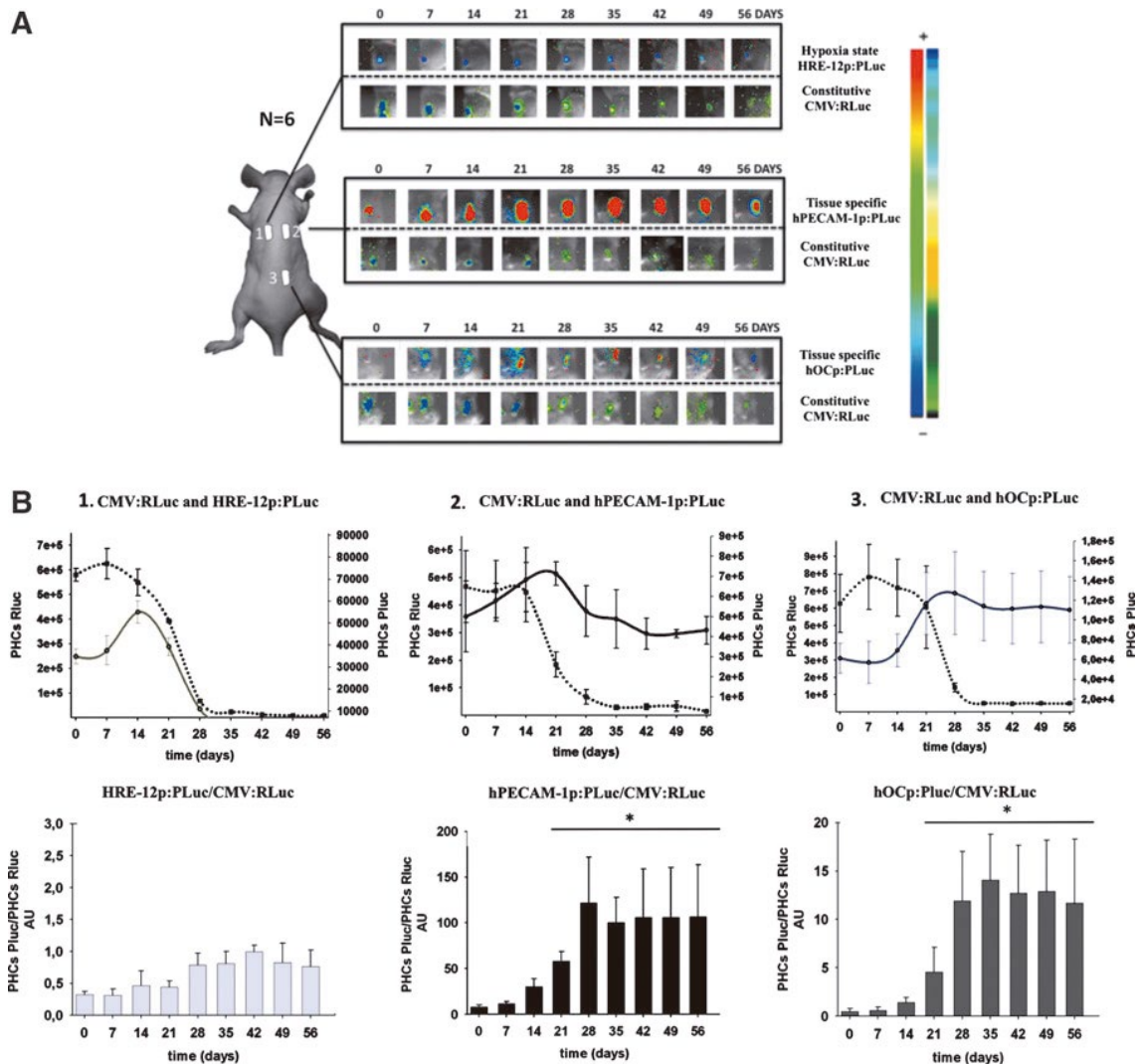
FIG. 2. Noninvasive BLI of hAMSC differentiation in subcutaneous implanted demineralized bone matrix (DBM) scaffolds. DBM scaffolds were subcutaneous implanted in the back of severe combined immunodeficiency (SCID) mice and seeded with hAMSCs previously transduced with the CMV:RLuc:mRFP reporter (a constitutively expressed reporter of cell number) and a cell differentiation reporter (PLuc:eGFP) regulated by hPECAM-1p, hOCp, or HRE-12p, and imaged at the indicated times. (A) Diagram illustrating the DBM implantation sites (numbered squares) and seeded cell types. Representative BLI and b&w composite images showing bottom row, RLuc; top row, PLuc, (n = 6). (B) (Top panel 1-3) Quantification of image data from (A). The graphs show average values for PHCs recorded in the images (RLuc regulated by CMV promoter, square symbol; PLuc regulated by specific promoter, round symbols). (Bottom panel 1-3) Histograms showing the ratio PLuc/RLuc calculated from photon fluxes recorded in BLI images. Arbitrary color bars represent light intensity levels for PLuc (blue, low; red, high) and RLuc (green, low; blue, high). *$p < 0.05$. HAMSC labeling scheme: DBM-1: PLox-HRE12p:PLuc:eGFP + CMV:RLuc:mRFP:ttk; DBM-2: PLox-hPECAM-1p:PLuc:eGFP + CMV:RLuc:mRFP:ttk; DBM-3: PLox-hOCp:Pluc:eGFP + CMV:RLuc:mRFP:ttk. Color images available online at www.liebertpub.com/tea

TABLE 1. *In Vivo PGK1/LDH, PECAM-1, and Osteocalcin Gene Expression*

21 days			42 days			56 days		
PGK1/LDHA	*PECAM-1*	*OC*	*PGK1/LDHA*	*PECAM-1*	*OC*	*PGK1/LDHA*	*PECAM-1*	*OC*
0/0	8.96	5.48	0/0	9.41	9.96	0/0	18.85	22.39

[a]Avarage C_t values from at least three independent experiments performed in duplicate were used to calculate fold changes in gene expression ($2^{-\Delta\Delta C_t}$) using *GADPDH* as reference.
OC, osteocalcin; PECAM-1, platelet endothelial cell adhesion molecule-1; PGK1, phosphoglycerate kinase 1; LDHA, lactate dehydrogenase.
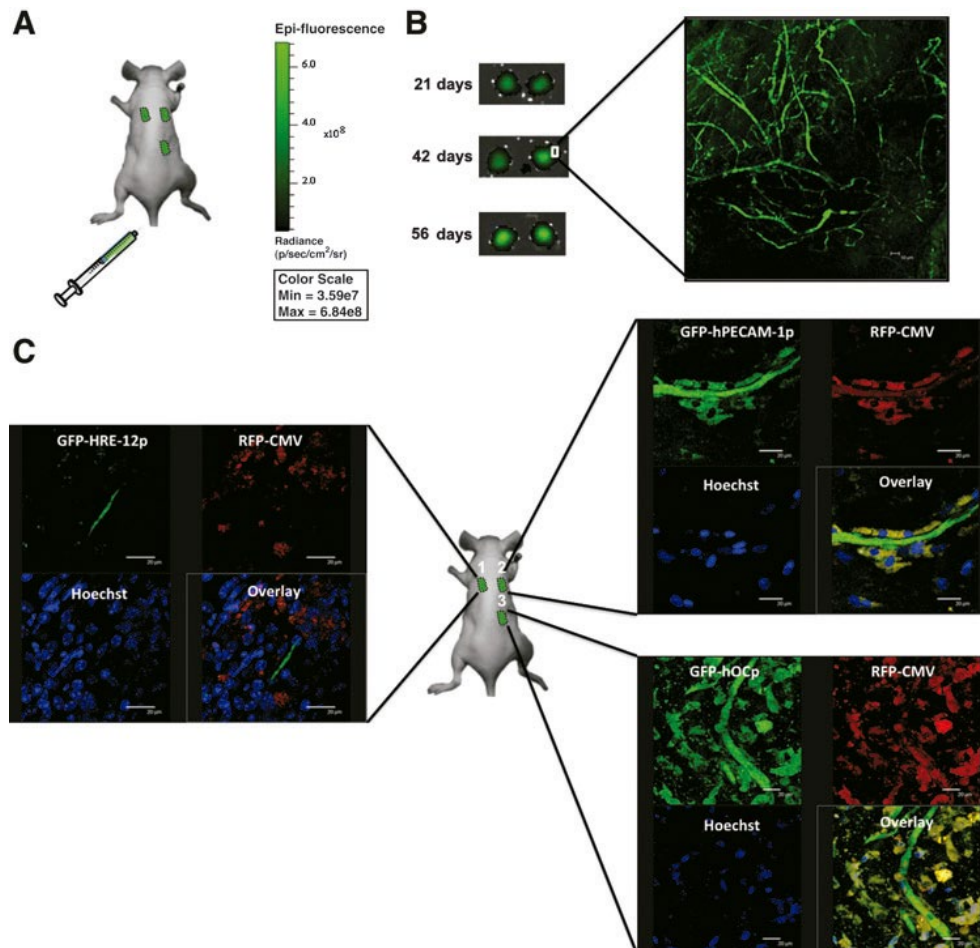

FIG. 3. Imaging of microvessel colonization of hAMSC-seeded DBMs in SCID mice. DBM-bearing mice were injected through the lateral tail vein with FITC-conjugated dextran (MW2,000,000 daltons). After fluorescent dextran perfusion, DBM implants were harvested, formalin fixed, and sectioned for laser confocal microscope imaging of microvascular structures. (A) Diagram illustrating FITC–dextran injection procedure. (B) Dextran-perfused DBM scaffolds harvested at the indicated times were imaged for dextran fluorescence using an IVIS spectrum (Caliper Life Sciences) (left), and by laser confocal microscopy at low (10 ·) magnification to reveal fluorescent microvascular networks within the DBM section (right) (Scale bar: 50 mm). (C) High-magnification (63 ·) images from dextran-labeled capillary network regions. Each set of images shows (top right) red fluorescent cells corresponding to the implanted hAMSCs present in all implants, (top left) cells expressing GFP regulated by specific promoter, and FITC-labeled microvessel (bottom left) Hoechst-stained nuclei, and (bottom right) red, blue, and green composite image (scale bars: 20 mm). Color images available online at www.liebertpub.com/tea
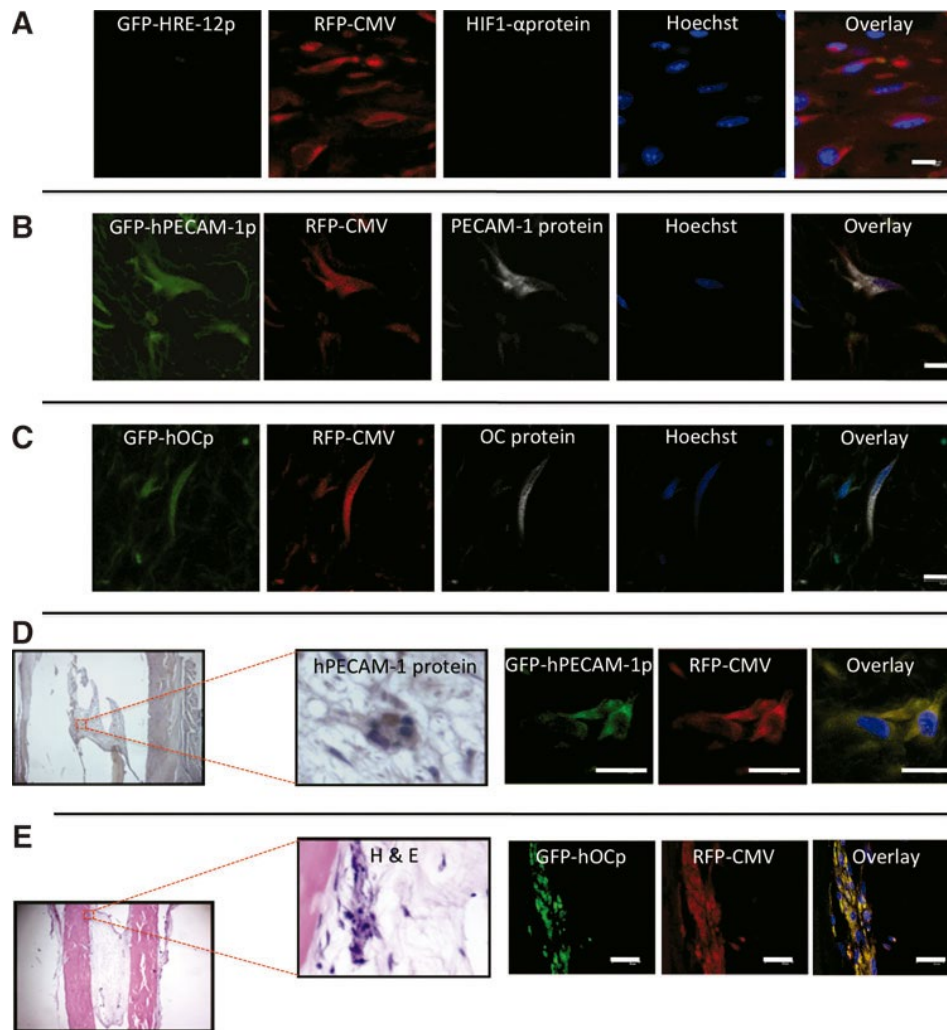
FIG. 4. Immunofluorescence staining, immunostaining, and staining for detection of specific proteins hPECAM-1, hOC, and HIF-a and bone formation in DBM-implanted hAMSCs. hAMSC-seeded DBM sections were imaged by laser confocal microscopy to reveal GFP and red fluorescent protein (RFP)-positive cells and then incubated with primary antibodies against HIF1-a (A), hPECAM-1 (B), or hOC (C), followed by a Cy5-conjugated secondary antibody (3 mg/mL; Jackson ImmunoResearch) and 4,6-diamidino-2-phenylindole (Hoechst, Sigma) for nuclear staining. In each row, images show, from left to right, green fluorescence protein regulated by tissue-specific promoter; RFP regulated by constitutively active CMV promoter in all implanted hAMSCs; specific ab-detection of the corresponding endogenous protein marker; Hoechst nuclear stain; and overlay of four images (scale bars: 10 mm). (D) From left to right, the panel shows hPECAM in vivo staining of a DBM section (· 5); higher magnification of the image showing positive hPECAM cells in capillary structure (· 80); cells expressing GFP regulated by PECAM promoter from parallel section; cells expressing RFP regulated by the CMV promoter from the same section; previous images merged with also Hoechst stained nuclei (blue). Scale bar: 10 mm. (E) From left to right, the panel shows hematoxylin and eosin (H&E)-stained DBM section (· 5); higher magnification of the same section showing cells positive for deposited calcium (· 20); cells expressing GFP regulated by hOCp, from parallel section; cell expression RFP regulated by the CMV promoter from the same section; previous two images merged with also Hoechststained nuclei (blue). Scale bar: 25 mm. (a) DBM-1. PLox-HRE12p:PLuc:eGFP + CMV:RLuc:mRFP:ttk. (b) DBM-2. PLoxhPECAMp: PLuc:eGFP + CMV:RLuc:mRFP:ttk. (c) DBM-3. PLox-hOCp:PLuc:eGFP + CMV:RLuc:mRFP:ttk. Color images available online at www.liebertpub.com/tea